Research Article

Late Pleistocene and Holocene aeolian activity in the Deliblato Sands, Serbia

György Sipos[a]* 🔾 , Slobodan B. Marković[b], Milivoj B. Gavrilov[b], Alexia Balla[a], Dávid Filyó[a], Tamás Bartyik[a],
Minucher Mészáros[b], Orsolya Tóth[a], Boudewijn van Leeuwen[a], Tin Lukić[b], Petru Urdea[c], Alexandru Onaca[c],
Gábor Mezősi[a] and Tímea Kiss[a]

[a]Geomorphological and Geochronological Research Group, Department of Geoinformatics, Physical and Environmental Geography, University of Szeged, H-6722 Szeged, Egyetem u. 2-6, Hungary; [b]Chair of Physical Geography, Department of Geography, Tourism and Hotel Management, University of Novi Sad, Trg Dositeja Obradovića 3, Novi Sad 21000, Serbia and [c]Department of Geography, West University of Timișoara, B-dul. Vasile. Parvan Nr. 4, 300223, Timișoara, Romania

Abstract

The Deliblato Sands is among the largest uniform dune fields of Europe, with a very pronounced topography reflecting extensive past aeolian events. Although lacking numerical age data, previous researchers have hypothesized various periods of dune formation. Our research goals were to map the main morphological units of the Deliblato Sands, and to provide the first optically stimulated luminescence (OSL) ages for the major dune types. Mapping was carried out using digital elevation models, satellite images, and GPS profiles. Dune development was investigated using OSL. Several tests were performed concerning thermal treatment, signal characteristics, dose recovery, and dose distributions to assess the suitability of sediments for luminescence dating. Based on our results, two dune generations could be identified that differed in morphology and age. Older dune forms are primarily low sand-supply, hairpin-like parabolic dunes that developed from the last glacial maximum until the end of the early Holocene, then became stabilized. Younger, superimposed parabolic dunes record an intensive aeolian signal from the eighteenth and nineteenth centuries. The history of the Deliblato Sands fits with those from other European sand dune areas, and provides further details to understand paleoenvironmental changes in the region.

Keywords: Deliblato Sands, Fixed sand dunes, Parabolic dunes, Late Pleistocene, Holocene, OSL, Serbia

(Received 9 February 2021; accepted 17 October 2021)

INTRODUCTION

The Carpathian Basin is particularly rich in aeolian landscapes, such as loess plateaus and dune fields. Dune fields were predominantly formed from fluvial deposits of the Danube, the Tisza, and other rivers during the dry and cold climatic phases of the Pleistocene (Borsy, 1990). When vegetation was scarce, winds could attack and erode former alluvial surfaces, alluvial fans, and terraces, which were abandoned due to avulsion or incision of major rivers (Bukurov, 1982; Gábris, 2003; Mezősi, 2017).

Other dune fields of the region, especially in Hungary, have been extensively studied in the past decades using various geomorphological and dating methods (Lóki, 1981; Borsy, 1991; Kiss et al., 2009, 2012a; Buró et al., 2016; Györgyövics and Kiss, 2016). The main phase of aeolian activity has been dated to the last glacial maximum (LGM) (Borsy, 1991) when, due to the lack of vegetation, dune forms could develop anywhere where sand was available. However, several pieces of evidence exist for renewed dune formation during the last glacial termination or late glacial (ca. 19–11 ka; Shakun and Carlson, 2010) and in the

Holocene (Nyári et al., 2007; Kiss et al., 2012b; Sipos et al., 2016). This phase of climate-driven aeolian activity lasted the longest on the driest, central and eastern parts of the Carpathian Basin (Mezősi, 2017).

There is minimal information concerning blown sand movement in the Deliblato Sands in Serbia, an area termed the 'Desert of Europe' or 'European Sahara,' because it is characterized by large, fixed dune forms that were bare in the past few centuries, and provided a desert-like look to the landscape until the beginning of the 20th century (Cholnoky, 1902). The development of the dune field has been investigated by several researchers in the past, and primarily based on geomorphic observations, various hypotheses and assumptions were made concerning the origin and the time of its formation (Cholnoky, 1910, 1940; Menković, 2013).

Based on the model of Bukurov (1954), development of the area is strongly related to Pleistocene climatic oscillations; namely, the sand was accumulated in the area by the Danube River in interglacials, and during dry glacials, repeated aeolian activity could have reworked the fluvial deposits. As the sand overlies loess at some locations, other authors placed the major deflation phase in the Holocene, subsequent to fluvial deposition and loess formation (Marković-Marjanovič, 1950). More recently, Menković (2013) concluded that the sand sheet was formed during the last glacial termination and the Preboreal (10.3–9 ka) and

*Corresponding author email address: <gysipos@geo.u-szeged.hu>

Boreal (9–8 ka) periods of the Early Holocene (Greenlandian stage), and, after an Atlantic period (8–5 ka) stabilization in the Mid Holocene (Northgrippian stage), the present-day dunes developed in the Subboreal period (5–2.5 ka) and later (Meghalayan stage). Nevertheless, it is essential to underline that no numeric age data were available when these hypotheses were formulated.

The clarification of the development of the dune field is important not only from a geomorphological aspect but since the dune forms record the direction of contemporary prevailing winds, dating of their formation can be the basis of reconstructing paleowind directions and temporal changes in regional atmospheric circulation patterns (Hesse, 2016; Gavrilov et al., 2018). Moreover, as aeolian landscapes are very sensitive, sand mobilization is then a good indicator of climatic and environmental change (e.g., Muhs and Holliday, 1995; Tolksdorf and Kaiser, 2012; Telfer and Hesse, 2013) and increased human impact (e.g., Kiss et al., 2009, 2012b; Hugenholtz et al., 2010).

Consequently, the central aim of our research was to determine the periods of aeolian activity in the Deliblato Sands by providing the first numerical age data that can then be used for further reconstruction of the region's Quaternary environment.

REGIONAL SETTING

The Deliblato Sands, with an area of 800 km^2, is the largest quasi-uniform dunefield in the Carpathian Basin, and it hosts some of the largest dunes known in the region. The oval-shaped dune field is bordered and eroded by the Danube in the SE, and it extends towards the NW to the floodplain of the Tamiš River (Fig. 1).

At present, the climate of northern Serbia and the study area itself is moderate continental, with cold winters and hot summers. The mean annual temperature is 11.1°C, and the mean annual precipitation is 606 mm (Gavrilov et al., 2018). If considering the De Martonne aridity index, the region's climate is semi-humid (Hrnjak et al., 2014). Prevailing winds in the Deliblato Sands blow with the greatest annual frequency (129.2 days) from the SE quadrant (Gavrilov et al., 2018), corresponding to the direction of the Košava, a regional wind with a diurnal character, generated by a pressure difference between the Mediterranean Sea and continental areas in Southern Russia and Bulgaria. The Košava can appear at any season, is usually not accompanied by precipitation, and is strengthened because of orographic influences (Unkašević et al., 2007). Based on recent studies, the Košava is the prevailing wind at present in this part of Serbia (Gavrilov et al., 2018), and presumably, it had a significant role in the past as well. Accordingly, both the form of the entire sand sheet and the dunes themselves are oriented in a SE–NW direction (Fig. 1, Fig. 2A).

The surface of the Deliblato Sands is composed of aeolian sand over an area of 350 km^2; the rest is covered by loess and loessic sediments (Fig. 1). Accordingly, the Deliblato Sands can be divided into a typical sand dune area in the SE and a transitional zone with loess cover in the NW. Loess was deposited on previously developed sand dunes and leveled out topographic differences (Zeremski, 1972; Fig. 1). At present, most of the area is forested; however, afforestation plans from the beginning of the nineteenth century showed that ~160 km^2 of bare, vegetation-free sand was exposed to severe deflation (Bachofen, 1815 in Mátyus, 1870), and stabilization of the blown sand took several decades (Roth, 1916). Consequently, most researchers claimed that dune forms must be a few centuries old (Menković, 2013).

Traditionally, the sand dune area of the Deliblato Sands has been separated into a so-called low (between 75 m asl and 135 m asl) and a high (up to 170 m asl) dune field (Bukurov, 1954; Fig. 2A). The low dune field developed on the former alluvial plain of the Danube and ramps up towards the high dune field in the NW. According to Menković (2013), the low dune field is characterized by 5–10 m-high elongated dune forms, with a length of a hundred to several hundred meters. The higher general elevation of the high dune field is explained by its development over a loess plateau (Menković, 2013). The area is comprised of dune forms with a relative height of 20–30 m and a length of up to a thousand meters.

METHODS

Mapping and sampling

Sites for sampling were selected based on 1) a digital elevation model (EU-DEM v11_E50N20), used for the identification of the main morphological units; 2) satellite images from Google Earth, used for mapping dune crests and locating different dune types; and 3) GPS profiles, taken in a SE–NW and a SW–NE direction to determine the relative height of dunes and to locate the exact sampling points (Fig. 2B). OSL sampling targeted the two major types of dunes identified in the accumulation zone of the dune field (Fig. 2B).

Two drillings were made at both sites, using either a hand drill with a drilling cylinder into which a 15-cm long, 5-cm diameter PVC tube could be fitted, or a RedHawk-type percussion drill. Samples were removed from the drilling head of the RedHawk drill under red LEDs in a black tent set up in the field. The first site was sampled on a large, filled, parabolic dune (a more detailed morphological description is provided later in this paper). One drilling was made on the slipface of the form (borehole D1/1; 44°54′03″N; 21°09′42″E) to determine the latest phases of dune formation, while the other was in the depression downwind of the dune (borehole D1/2; 44°54′05″N; 21°09′39″E) to get an idea on the timing of preceding aeolian events (Fig. 2). A somewhat similar strategy was followed in terms of the second site, but the first drilling was made on the crest of the form (borehole D2/1; 44°54′39″N; 21°05′03″E), and the second was made in an interdune depression (borehole D2/2; 44°54′41″N; 21°05′05″E) between two hairpin-like dune arms (Fig. 2). In both sites, boreholes were sampled for OSL dating at approximately every meter, taking into account changes in stratigraphy. Site one had 8-m-deep boreholes and site two had 5-m-deep boreholes. Cores were also described macroscopically, and thirteen OSL samples representing the major sedimentary units were selected for further analysis.

Luminescence Dating

Preparation of samples followed usual laboratory techniques (e.g., Mauz et al., 2002). All procedures were carried out in subdued yellow light provided by low-pressure sodium lamps. Selected samples were dried out, and the 90–150 μm fraction was separated out by dry sieving. Carbonate and organics were removed by repeated treatment in 10% HCl and 10% H_2O_2. Separation of the quartz fraction was made using heavy liquid flotation (LST Fastfloat). Finally, a 45-minute etching in 40% HF was performed to remove any remaining feldspar contamination and the outer layer of quartz grains.

The equivalent dose (D_e) of samples was determined on a Risø DA-20 TL/OSL-type luminescence reader equipped with a
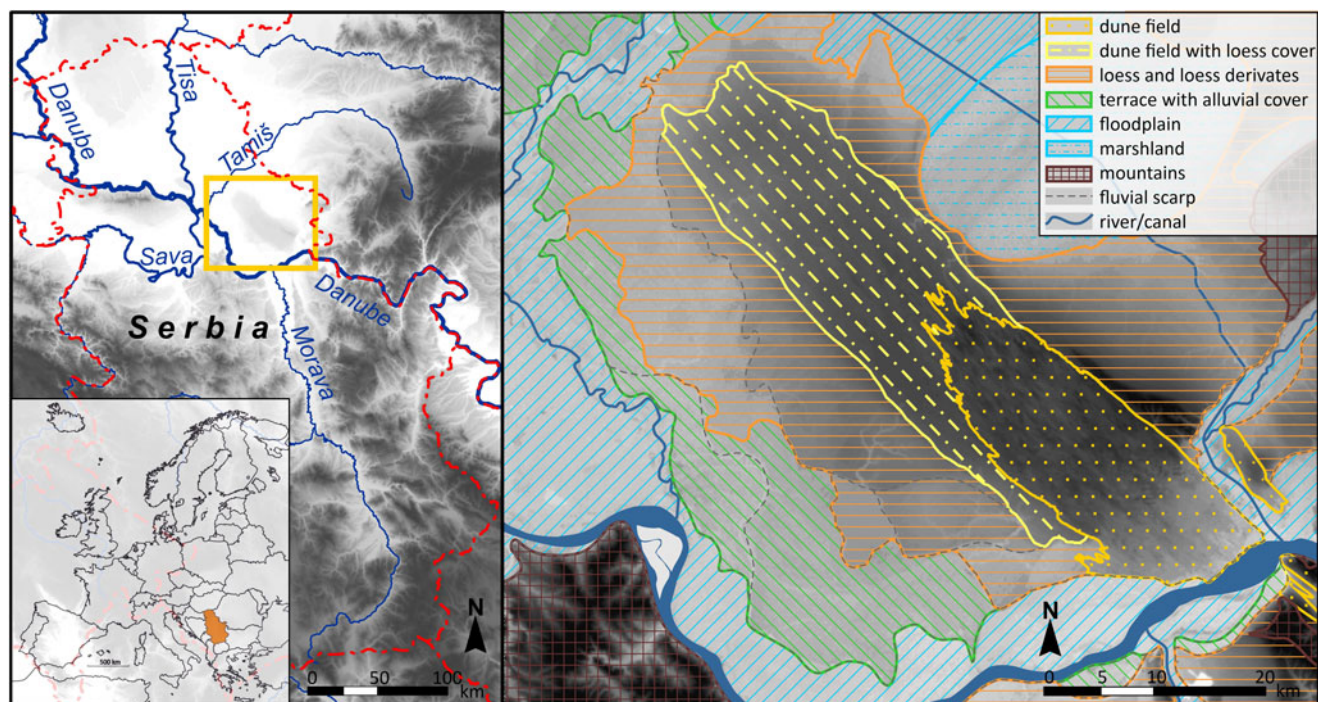
Figure 1. The location of the Deliblato Sands in Europe and the geomorphology of its surroundings. Small inset map on bottom left shows Serbia shaded in; square in larger map on left shows approximate study area; area inside square is shown in detail in map on right.

$^{90}SR/^{90}Y$ β-source and an EMI ET9107-type photomultiplier (Bøtter-Jensen et al., 2010). Stimulation was carried out using blue (470 ± 30 nm) LEDs set for 90% power release, while detection was made through a Hoya U-340 filter. Throughout the measurements, the single aliquot regeneration (SAR) protocol was applied (Murray and Wintle, 2003; Wintle and Murray, 2006). Prior to SAR tests, some of the samples were subjected to an LM-OSL analysis to resolve the components of the OSL signal and to determine the ratio of the fast component (Bulur, 1996; Jain et al., 2003; Singarayer and Bailey, 2003), that is usually low in Danube sediments (Bartyik et al., 2021). Subsequently, preheat and dose recovery tests were performed to identify the optimal measurement parameters and assess the reproducibility of measurements. The effect of applying an elevated temperature OSL treatment at the end of SAR cycles was also tested because its application on other Danube-related sediments caused a considerable decrease in measurement reproducibility as a matter of thermal transfer (Tóth et al., 2017). Additionally, the effect of aliquot size on D_e distribution was also tested.

During OSL measurements, optical stimulation was performed at 125°C (heating rate: 5°C/s) for 40 seconds. Standard rejection criteria were used to select aliquots that performed well during the SAR measurements (Murray and Wintle, 2003). Potential feldspar contamination of the quartz extracts was monitored by the IR/OSL depletion ratio, as proposed by Duller (2003). In the case of each sample, at least 24 aliquots were analyzed. The ratio of aliquots passing the rejection criteria was 90% on average when using a 6-mm mask size. Dose-response curves were fitted in each case using the sum of two saturating exponential functions: $I(D) = I_0 + A(1-exp^{(-D/D01)}) + B(1-exp^{(-D/D02)})$.

Single-aliquot D_e values were plotted on abanico plots (Dietze et al., 2016) generated in the R luminescence package (Kreutzer et al., 2012). Sample D_e values were calculated using either the CAM or the MAM age model of Galbraith et al. (1999). A

decision between the two was made using the single aliquot threshold values proposed by Arnold et al. (2007), which are obtained based on the skewness (c), kurtosis (k), overdispersion (σ), and the coefficient of variation (CV) of dose distributions.

Environmental dose rate (D*) was determined using high-resolution, extended-range gamma-ray spectrometry (Canberra XtRa Coaxial Ge detector). Dry dose rates were calculated using the conversion factors of Liritzis et al. (2013). Attenuation factors for β dose rates were given after Brennan (2003). Wet dose rates were assessed based on in-situ water contents (Aitken, 1985). The rate of cosmic radiation was determined by considering burial depth, and geographic location, following the equation of Prescott and Hutton (1994).

RESULTS

Morphological units and dune forms

In total, 1322 dune crests were mapped by thoroughly screening satellite images. Although this 2-D approach is not the most appropriate technique to survey dune forms, especially on areas under partial forest cover, by complementing the mapping with available low-resolution DEM and field observations, the major geomorphological units and dune types of the Deliblato Sands could be identified. Using these techniques, the traditional morphological map of the area was refined (Fig. 2B), and dune forms could be reclassified.

Accordingly, the low dune field of the Deliblato Sands can be separated morphologically into deflation and transportation zones (Fig. 2B). Deflation areas are characterized by blowouts, planar surfaces, and a low density of positive forms, being mostly blow-out dunes and residual ridges. In the transportation zones, elongated positive forms can be identified, with maximum lengths of 100–200 m, and a height of 3-4 meters. Therefore, the SE quarter
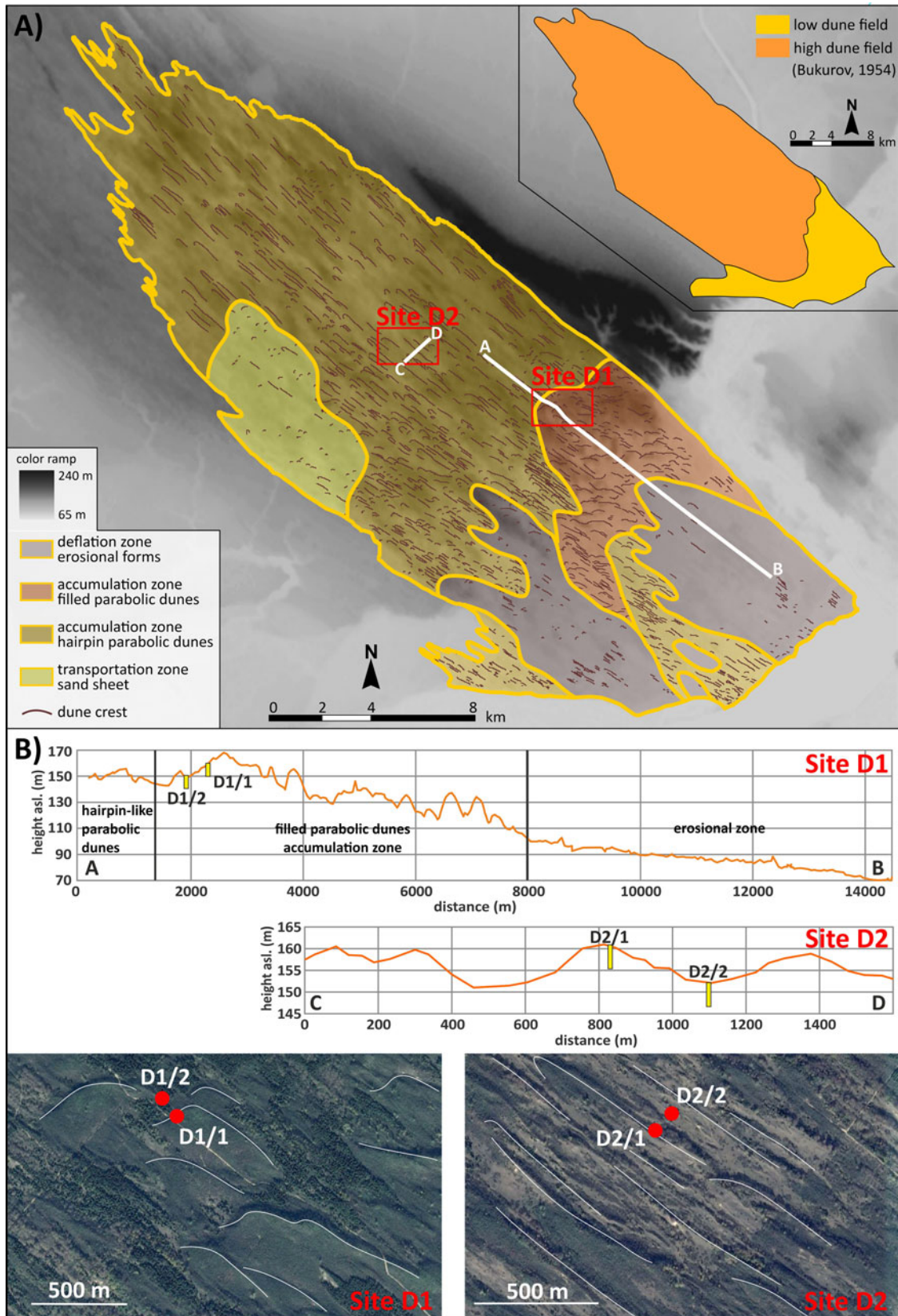
Figure 2. (A) The geomorphological zones of the Deliblato Sands (after Bukurov, 1954) with geomorphological units reinterpreted based on dune mapping, location of sampling sites, and tracks of GPS surveys labeled A–B (Site D1) and C–D (Site D2). (B) Position of drilling points on the surveyed topographic profiles, and satellite image subsets showing where cores were taken.

of Deliblato Sands can be interpreted as a potential source area for the northwesterly situated giant dunes located downwind.

The high dune field can also be separated into different zones based on the number and dimension of the mapped dunes (Fig. 2A). The easternmost area is interpreted as a high sand supply accumulation zone, with dunes up to a 20–25 m relative height. The crest of these dunes is slightly curved and their length is 0.5–1 km (Fig. 2). In some places, they resemble the transverse dunes of deserts, but they can instead be classified as filled parabolic dunes, indicating an abundant sand supply that can be easily explained by the proximity of a large sand source. The wind direction attributed to their formation is more southerly than the present direction of the southeasterly Košava (see Gavrilov et al., 2018).

Northwest of the previous zone, a lower sand supply accumulation zone that occupies the most extensive area on the dune field can be identified with a complex association of smaller, 5–10-m-high elongated dunes, blowout depressions, and residual ridges (Fig. 2A). The southwest part of this zone is characterized by many smaller blowout dunes that transform into parabolic dunes with elongated arms. Consequently, most longitudinal forms can be interpreted as left-behind wings of hairpin-like parabolas, indicating a moderate sand supply and considerable vegetation control during dune formation. The length of these parabolic dune arms is typically a few hundred meters, but in some places, they can reach a length of 1–1.5 km. Based on dune crests orientations, the wind direction during dune formation was $117 \pm 6°$, coinciding with the modern prevailing wind regime (Gavrilov et al., 2018). Finally, there is a zone dominated by sand transportation at the western part of the dune field with a low number of identifiable dune forms (Fig. 2A).

Luminescence properties

The luminescence performance of quartz extracts was first tested by applying a linearly modulated (LM) OSL measurement on one of the samples, using 2-mm aliquots. Although the selected sample was one with a considerable equivalent dose, due to its very low natural signal, components could not be entirely resolved. Therefore, the regeneration LM-OSL signal in response to ~20 Gy was analyzed in more detail (Supplemental Figure 1). In total, six components could be separated, including one fast, one medium, and four slow components. No ultrafast component was identified, and the dominance of the fast component in the initial part of the signal was overwhelming (Supplemental Figure 1). Thus, the signal properties of Deliblato quartz are adequate when the signal is strong enough, i.e., when the paleodose is high or large aliquots are used for the measurements.

Consequently, combined preheat and dose recovery tests were made using 6-mm aliquots. Recycling ratios were good up to 260°C, while recuperation usually showed a continuous increase, and from 280°C, it crossed the 5% rejection threshold (Supplemental Figure 2). Because of these results, and based on the findings of Tóth et al. (2017), special attention was given to dose recovery ratios and the effect of 280°C cleanouts (hot bleach) at the end of the SAR cycles. Elevated temperature treatment improved recycling ratios to some extent, but decreased the reproducibility of measurements because dose recovery ratios showed a higher scatter and were farther from unity than in case of tests where hot bleach was not inserted (Supplemental Figure 2).

By applying a preheat and a cutheat temperature of 220°C and 160°C, respectively, dose recovery tests were extended to 24 aliquots per sample, again by including and excluding cleanouts at the end of SAR cycles (Supplemental Figure 3). The application of an elevated temperature treatment caused a significant underestimation of dose recovery ratios. Values were near the 0.9 threshold suggested by Murray and Wintle (2003). Measurements without such a treatment produced mean results very close to unity (Supplemental Figure 3). Consequently, no elevated temperature cleanout was applied for subsequent tests and during the measurement of equivalent doses.

Continuous wave (CW) OSL decay curves, similarly to LM-OSL results, also indicated the moderate sensitivity of samples. By increasing aliquot size from 2 mm (~180 grains) to 6 mm (~1600 grains), signal intensity was considerably improved (Fig. 3). This way, the proportion of aliquots passing SAR rejection criteria increased to 90%.

Single-aliquot dose distributions

Although larger aliquot size meant better turnout rates in terms of the measurements, aliquot-to-aliquot scatter was also reduced, and information on the sedimentation history of grains might have been lost. This issue was important because proximity of the fluvial sediment source raised the matter of incomplete natural bleaching and potential age overestimation.

Because of the low luminescence sensitivity of samples, we assumed that 2-mm aliquots carry only a restricted number of luminescent grains, and are just appropriate to detect asymmetric sample D_e distributions indicating incomplete natural bleaching (Fig. 4). However, when comparing single aliquot D_e distributions measured from the same sample but using different aliquot sizes, we found that statistical parameters describing the width of the distribution (σ and CV) stayed similar throughout the test. In contrast, those describing the asymmetry and the tail of the curve (c and k) were increased by the presence of some high-residual outlying aliquots (Fig. 4). Therefore, we found that applying medium-sized (6-mm) aliquots would not lead to significant information loss in terms of D_e scatter.

Concerning the D_e distribution of samples measured using 6-mm aliquots, statistical parameters showed a limited variation in most cases (Supplemental Table 1). If considering the threshold values of Arnold et al. (2007), four samples had a statistically significant c and k score, while except for one sample (D2/1-300) σ and CV values were far less than the 40% threshold proposed by them for both parameters. Thus, from this aspect, the width of distributions was below the proposed limit. Still, D_e was determined using the MAM (minimum) age model for these samples. The CAM (central) age model was applied to the rest of the samples (Galbraith et al., 1999). When looking at abanico plots, increased asymmetry and the narrowness of the dose distributions are the consequence of one or two outliers at the higher end of the values (Supplemental Figure 4). Thus, in the case of three samples of the four affected, MAM and CAM age models yielded very similar D_e values, while in the case of sample D2/1-300, the difference was 13% (Supplemental Table 1). Consequently, we determined that the aeolian samples of the Deliblato Sands are relatively well-bleached, and fluvial origin affects dose distribution for only a few samples (Supplemental Figure 4).

Profiles and OSL ages

Based on mapping results, the sampled dune at Site D1 is a filled parabolic dune, indicating an abundant sand supply and limited
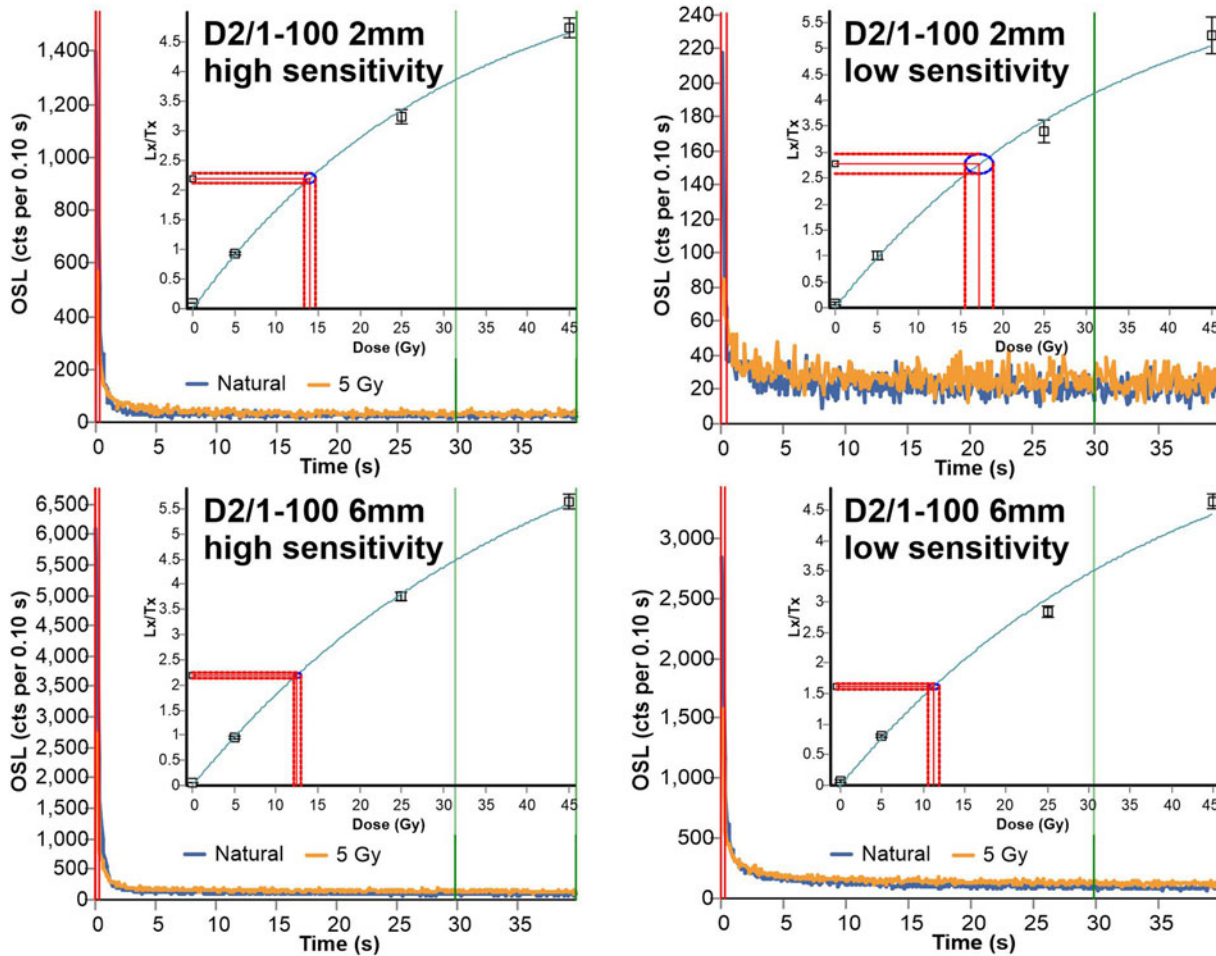
Figure 3. Typical optically stimulated luminescence (OSL) decay curves and dose-response curves at 2-mm- and 6-mm aliquot size, representing both low and high sensitivity aliquots of the same sample D2/1-100.

vegetation control during its formation. Its relative height is 19 m, and the length of its crest is 750 m. The 8-m-deep borehole D1/1 from its slipface recovered homogenous, pale yellow, medium grain-sized dune sand (Fig. 5). The sand in the entire section was dated to 0.2 ka, indicating that dune formation stopped around the beginning of the nineteenth century (Table 1).

A more complex stratigraphy and chronology were found at the base of dune D1 (borehole D1/2; Fig. 5). The lowermost layer of blown sand at a depth of almost 8 m was dated to the Younger Dryas (sample D1/2-780, 12.50 ± 0.71 ka; Fig. 5). Within next the sand layer above to approximately a depth of 3 m, several horizons of carbonate concretions (from 0.5 cm to 4 cm in size) were found, indicating increased evapotranspiration at the time of their formation (Li et al., 2018). The upper part of the sedimentary unit was dated to the very end of the Younger Dryas period (sample D1/2-480, 11.05 ± 0.66 ka). At a depth of 5 m, a thin calcareous clayey, silty layer was identified, which indicates a short pause in dune formation in accordance with the obtained OSL ages.

Over the Younger Dryas blown sand layer, a thin (10–15 cm) organic-rich horizon was found that was overlain by a 60–70 cm-thick silty-to-clayey carbonate-rich unit (Fig. 5). This sequence suggests a marshy environment in a local depression that changed into an area with temporary water cover, leading to the accumulation of fine calcareous sediments. Carbonate mobilization by water and regular desiccation of the area could also have led to the development of the carbonate concretion-rich horizons below. Based on numerical ages from the profile, this period of deposition is estimated to have occurred in the Preboreal period of the Holocene. The carbonate-rich unit is overlain by another 2-m-thick blown sand unit dated to 8.72 ± 0.65 ka (sample D1/2-100), suggesting a notable Boreal aeolian event (Fig. 5, Table 1).

The dune form at Site D2 has a relative height of 8 m, considerably lower than the previously described dune. The elongated form is 800 m in length, and is interpreted as the arm of a hairpin-like parabolic dune that developed under substantial vegetation control and a moderate sand supply. Borehole D2/1, drilled on the crest of the form, recovered medium grain-sized dune sand with two carbonate-rich horizons (Fig. 5). Most probably, the core of the dune started to develop during the Older Dryas period (sample D2/1-500, 14.58 ± 0.82 ka) and heightened gradually, as indicated by an OSL date from a depth of 3 m that shows a Preboreal period of sand deposition (Table 1). Above the calcareous horizons, Boreal-age blown sand was found (sample D2/1-100, 8.24 ± 0.57 ka), and secondary carbonate concretions, detected below, most likely developed in this period (Fig. 5). These results indicate a moderate rate of sand transport
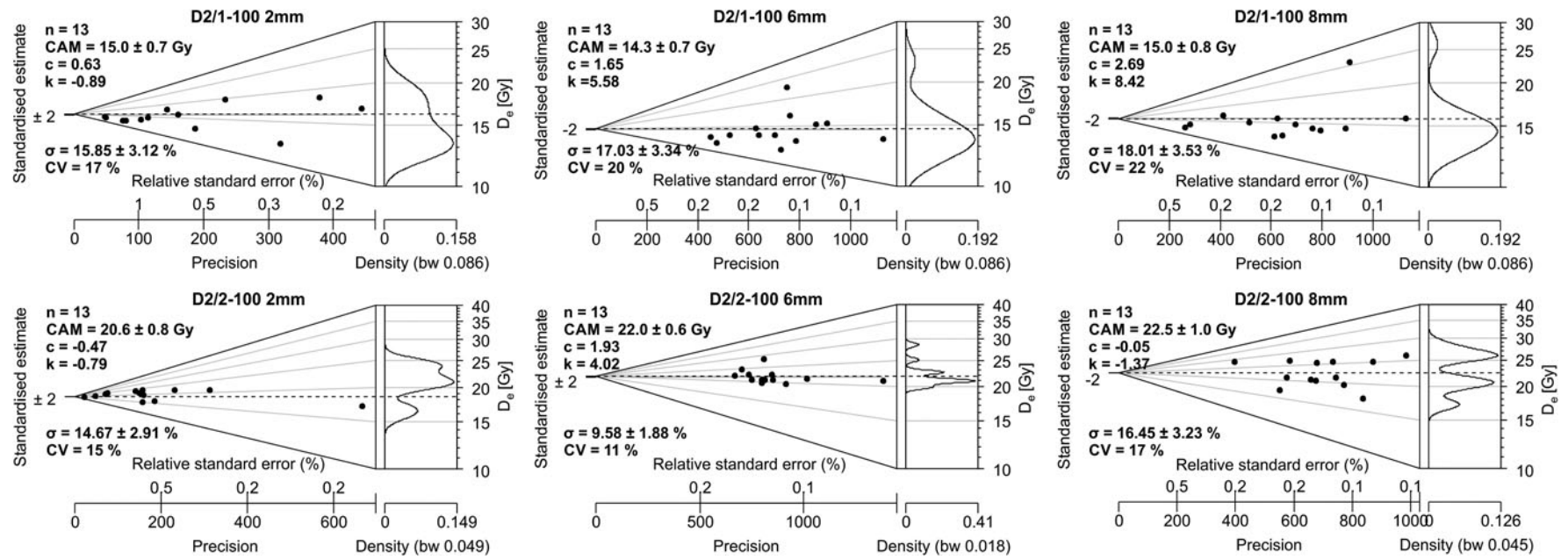
Figure 4. Abanico plots (see Dietze et al., 2016) and statistical parameters of single aliquot D_e results (σ: overdispersion value, c: skewness, k: kurtosis), measured using different mask sizes. For 2-mm aliquots, 13 out of 24 aliquots passed single aliquot regeneration (SAR) criteria in both cases. Accordingly, the first 13 measurements (n) were plotted in the case of larger aliquots with a better turnout rate.
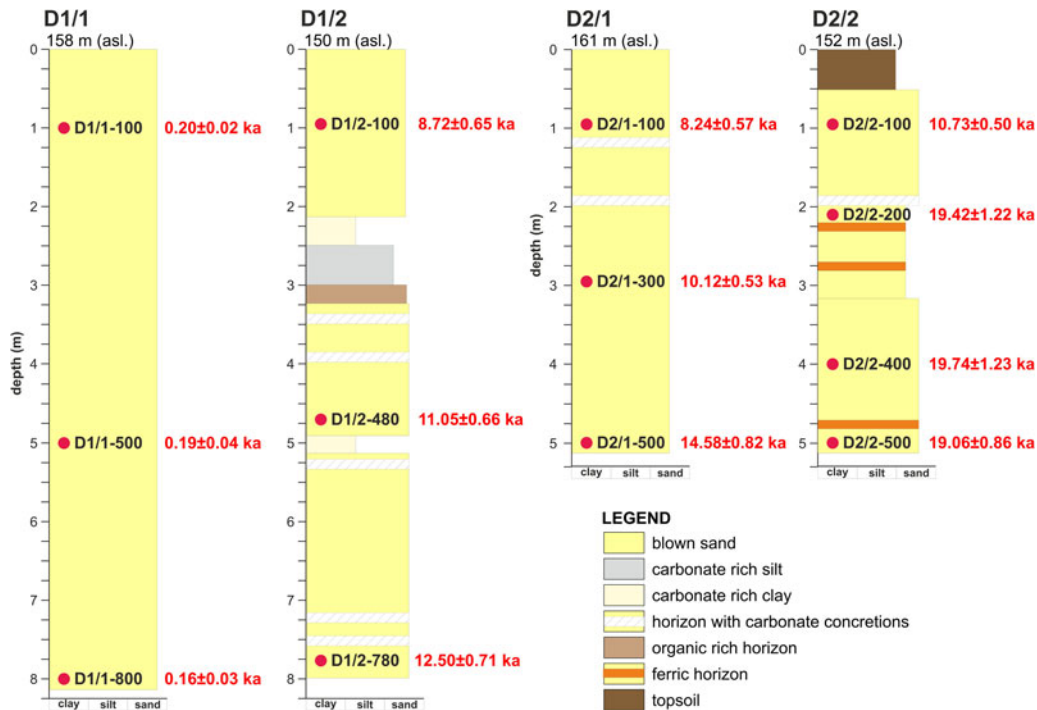
Figure 5. Stratigraphy and optically stimulated luminescence (OSL) ages of sediment samples from boreholes made at sites D1 and D2 (see Figure 2B for relative locations), representing a filled parabolic dune and a hairpin-like parabolic dune, respectively.

Table 1. Optically stimulated luminescence (OSL) ages and data used for age calculations; w: in-situ water content; D*: total dose rate; D_e: sample equivalent dose based on data in Supplemental Table S1.

Sample ID and depth (cm)	w (%)	^{238}U (ppm)	^{232}Th (ppm)	K (%)	D* (Gy/ka)	D_e (Gy)	Age (ka)
D1/1-100	3 ± 2	1.37 ± 0.11	3.41 ± 0.32	1.10 ± 0.03	1.75 ± 0.05	0.35 ± 0.04	0.20 ± 0.02
D1/1-500	4 ± 2	1.25 ± 0.10	3.92 ± 0.37	1.08 ± 0.03	1.65 ± 0.06	0.32 ± 0.06	0.19 ± 0.04
D1/1-800	5 ± 2	1.28 ± 0.11	3.82 ± 0.34	1.09 ± 0.03	1.62 ± 0.06	0.26 ± 0.04	0.16 ± 0.03
D1/2-100	6 ± 2	1.30 ± 0.11	3.72 ± 0.27	1.09 ± 0.03	1.69 ± 0.07	14.77 ± 0.93	8.72 ± 0.65
D1/2-500	4 ± 2	1.30 ± 0.11	3.72 ± 0.35	1.09 ± 0.03	1.64 ± 0.06	18.14 ± 0.87	11.05 ± 0.66
D1/2-780	5 ± 2	1.28 ± 0.11	3.92 ± 0.03	1.08 ± 0.03	1.61 ± 0.05	20.16 ± 0.95	12.50 ± 0.71
D2/1-100	7 ± 5	1.47 ± 0.10	3.85 ± 0.32	1.02 ± 0.02	1.68 ± 0.08	13.72 ± 0.68	8.24 ± 0.57
D2/1-300	8 ± 5	1.47 ± 0.10	3.85 ± 0.32	1.02 ± 0.02	1.64 ± 0.08	16.47 ± 0.37	10.12 ± 0.53
D2/1-500	7 ± 5	1.47 ± 0.10	3.85 ± 0.32	1.02 ± 0.02	1.61 ± 0.08	23.53 ± 0.67	14.58 ± 0.82
D2/2-100	8 ± 5	2.09 ± 0.14	5.44 ± 0.39	1.18 ± 0.03	2.05 ± 0.08	21.95 ± 0.55	10.73 ± 0.50
D2/2-200	20 ± 5	1.51 ± 0.12	4.75 ± 0.37	1.19 ± 0.03	1.67 ± 0.06	32.41 ± 1.6	19.42 ± 1.22
D2/2-400	17 ± 5	1.80 ± 0.10	5.15 ± 0.34	1.23 ± 0.03	1.80 ± 0.06	35.53 ± 1.76	19.74 ± 1.23
D2/2-500	12 ± 5	2.28 ± 0.15	6.20 ± 0.44	1.46 ± 0.03	2.07 ± 0.07	39.5 ± 1.25	19.06 ± 0.86

and a slow but almost continuous development of the dune form up to the Atlantic period.

In the blowout hollow parallel to the dune, LGM deposits were recovered from borehole D2/2 at depths between 5 m and 2 m (Fig. 5). The mean value of ages was 19.4 ka (Table 1). The 3 m-thick sand contained three thin, ferric horizons, indicating groundwater fluctuation and an oxidative environment during the development of these horizons. From a depth of 3 m, medium sand was replaced by fine sand, i.e., it is likely that wind strength

had generally decreased. The LGM sand deposit is covered by an almost solid calcareous horizon, above which an early Holocene (sample D2/2-100, 10.73 ± 0.50 ka) sand layer was found (Fig. 5, Table 1). Deposits in D2/1 and D2/2 profiles suggest that the erosion of the blowout and the accumulation of the dune body mainly occurred during the Preboreal period. Their formation possibly lasted until the end of the Boreal period, when the dune was still growing and presumably the hollow was also developing. Based on these data, it is suggested that the development of the soil in

the depression started in the Atlantic period, and since then, no severe wind erosion has occurred.

DISCUSSION

Based on the four dated profiles at two sites, the main phases of the aeolian activity in different parts of the Deliblato Sands could be reconstructed, and a brief history of development outlined for the past 20 ka. Moreover, for the first time, phases of Deliblato dune formation can be compared to those identified at other sand dune areas of the Carpathian Basin and Europe, and related to available paleoclimatic information.

Although LGM-age sand was only found at the base of the investigated hairpin-like parabolic dune (samples D2/2-500, D2/2-400, D2/2-200), dune formation was probably active throughout the entire dune field at this time, which is also supported by data available from other sand dune areas of the Carpathian Basin (Kiss et al., 2012b; Buró et al., 2016; Györgyövics and Kiss, 2016) and key sites of cover sands in northwest and western Europe (Kasse, 2002; Vandenberghe et al., 2013; Bertran et al., 2013). According to the regional climate reconstruction of Ludwig et al. (2021), based on malacological data, the LGM can be characterized by a semiarid climate; however, in the summer months (JJA), and especially in the southeast part of Vojvodina where Deliblato Sands is situated, conditions were relatively arid in contrast to the present-day humid and semi-humid climatic regime (Hrnjak et al., 2014). Under these circumstances, there were highly favorable conditions for extensive dune formation.

Geomorphic and climatic evidence suggest that environmental conditions during the Oldest Dryas (17.5–14.7 ka; INTIMATE event GS-2.1a of Rasmussen et al., 2014) were still favorable for sand movement, as indicated by luminescence ages obtained at other Carpathian Basin dune fields (Novothny et al., 2010; Kiss et al., 2012a; Buró et al., 2016). The interpretation of a cold and dry climate in the region is also reinforced by the occurrence of sand wedges 250 km to the north that date to this period (Fábián et al., 2014), and CCSM3 model-based climate simulations (Collins et al., 2006; Fordham et al., 2017). However, at the sites investigated in the present study, only one sample represents this period (sample D2/1-500), with the next major phase of aeolian activity after the LGM dated to the Younger Dryas and the Preboreal.

Following the climatic amelioration during the late glacial Bølling-Allerød warming (14.7–12.9 ka, GI-1 INTIMATE event of Rassmussen et al., 2014), the Carpathian Basin region was generally characterized by an overall cooling at the onset of the Younger Dryas (Feurdean et al., 2008). However, based on pollen and Chrinomidae records, the temperature decrease was subtle compared to the climatic perturbation in the North Atlantic (Sümegi et al., 2011, 2013; Tóth et al., 2012), and this was especially true in lowland areas and for summer (JJA) mean temperatures, which only decreased by <1°C on the NE parts of the Hungarian Great Plains (Magyari et al., 2019). There also was a marked drop in precipitation in Eastern Europe as indicated by several proxy records (Feurdean et al., 2014); thus, aridity increased significantly. By the onset of the Holocene, temperature significantly increased (Magyari et al., 2019), and according to the pollen-based reconstruction of Mauri et al. (2015), dry conditions persisted until ca. 9 ka in Europe. In southeast Europe, winter (DJF) precipitation was especially low in this period. Consequently, these conditions resulted in extensive deflation and blown sand movement in the Deliblato Sands during the Younger Dryas and the Early Holocene as indicated by four

samples (D1/2-780, D1/2-480, D2/1-300, D2/2-100) representing three of the four drilling sites. There are also several OSL-supported data on aeolian activity from this period from other dune fields of the region (e.g., Ujházy et al., 2003, Kiss et al., 2012b). Moreover, Younger Dryas/Preboreal dune formation has been widely reported from the area of the European Sand Belt (Hilgers, 2007, Tolksdorf and Kaiser, 2012, Kalińska-Nartiša et al., 2016, Moska et al., 2021), the inland deposits of the Iberian Peninsula (Bernat Rebollal and Pérez-González, 2008), and the coversands of the Atlantic coast in southwest France (Bertran et al., 2013).

Hence, it seems that a significant dune formation period can be identified in the study area between 12–10 ka, and at least 4 m of deposition can be attributed to this period at Site 1. Whether borehole D1/2 penetrates a Younger Dryas sand sheet filling up a depression, which could be inferred from the development of carbonate-rich horizons, or it intersects the sand of the dune downwind, which is suggested by its morphology (Fig. 2B, Fig. 5), it seems likely that dune forms were probably smaller in this area during the Younger Dryas than those formed more recently. This also means that a significant amount of material was deposited subsequently, resulting in relative dune heights of 20–25 m at Site 1, whereas at Site 2, dunes reach a maximum height of 5–10 m.

Another significant observation that can be made based on the results is that the main formation period of elongated parabolic dunes in the NW part of Deliblato Sands can be dated back to the late Glacial and Early Holocene; thus, they are significantly older than expected based on previous hypotheses (Marković-Marjanovič, 1950; Menković, 2013). This also means that the landscape was relatively stable in this part of the dune field for most of the Holocene. In this sense, the northern part of the Deliblato Sands resembles a similar sequence of aeolian events as the dunes in the Nyírség in NE Hungary (Buró et al., 2016; Kiss et al., 2012b).

At both study sites, Boreal-age deposits were also identified, either in an interdune depression (borehole D1/2) or on the top of a dune (borehole D2/1), indicating that overall aeolian activity probably lasted until 8 ka in the Deliblato Sands (samples D1/2-100, D2/1-100). From a paleoenvironmental perspective, dune stabilization occurred due to the encroachment of vegetation, which was enabled by a considerable increase in precipitation from 9 ka to 7 ka (DJF: 10–15 mm/month, JJA: 5–10 mm/month), as shown by the pollen-based reconstruction of Mauri et al. (2015). A marked shift to a negative NAO phase, accompanied by an intensifying Mediterranean cyclone activity and an increase in precipitation from 8.2 ka was found to occur in the region based on ice core $\delta^{18}O$ data from the Scărișoara Ice Cave, 200 km to the NE from Deliblato Sands (Perșoiu et al., 2017). On other sand dune areas of the Carpathian Basin, signs of Boreal-age aeolian activity have also been identified (Borsy, 1991; Nyári et al., 2007; Buró et al., 2016), but these are usually interpreted as events producing secondary blowouts on previously formed dunes (Borsy, 1991). Meanwhile, based on the extensive review of Tolksdorf and Kaiser (2012), aeolian activity in the European Sand Belt ceased later, at ca. 7 ka.

Both for the dune fields of the Carpathian Basin and those elsewhere in Europe, numerous previous studies indicate aeolian activity in the wet phases of the Middle and Late Holocene, referring to an increased human impact, leading to the deterioration of vegetation cover and the simultaneous start of deflation (e.g., Ujházy et al., 2003; Hilgers, 2007; Kiss et al., 2012b; Sipos et al.,

2016; Moska et al., 2021). Nevertheless, no such signs have been detected so far in the Deliblato Sands, which could be either due to low disturbance as a result of low population density in the area or because at least on the SE part of the high dune field, the record is overwritten by eighteenth-century dune formation. Based on the general geomorphologic picture, the elevation profiles measured, and the OSL ages obtained, it seems that filled parabolic dunes, formed in the past few centuries, were climbing up on the previously formed late Glacial/Early Holocene dune field. Also, as indicated by the findings of Gavrilov et al. (2018), both the amount of sand supply and the direction of the wind were different in terms of these forms as compared to hairpin-like parabolic dunes in the northwest portion of the dune field. The observations also serve to emphasize the fact that the two main accumulation zones of the high dune field have had different development histories.

CONCLUSIONS

With the help of morphological mapping and OSL dating of dune forms on the Deliblato Sands, novel information was obtained concerning the Late Pleistocene and Holocene evolution of the area, contributing to the regional interpretation of the contemporary aeolian record as well.

Based on the morphology and heights of the dunes, most of the dune field is dominated by elongated, hairpin-like parabolic dunes, indicating a relatively low sand supply during their formation. However, another set of dunes, predominantly a filled parabolic-type, are superimposed on the previous dunes and indicate a much higher sand supply.

According to the numerical ages obtained, the sand forming the base of the present dunes was deposited during the cold and arid LGM, until ca. 19 ka. Subsequently, another major phase of dune formation took place from the Younger Dryas to the Boreal period of the Holocene. However, due to increasing precipitation after 8 ka, the dune landscape was stabilized by vegetation. Therefore, on most of the Deliblato Sands, the dunes are older and more stable than previously assumed. In addition, Middle Holocene stabilization of dunes started earlier here and in the Carpathian Basin as compared to the European Sand Belt.

On the southeast portion of the high dune field, sand was remobilized during historical times. As indicated by our research, the last phase of aeolian activity was dated to 0.2 ka, which corresponds well with written records. Nevertheless, earlier events in historical times that are regularly observed on other European dune fields cannot be ruled out, even though the young dune forms are directly superimposed on the late Glacial to Early Holocene deposits based on their geomorphological position and obtained OSL ages.

REFERENCES

Aitken, M.J., 1985. *Thermoluminescence Dating*. Academic Press, London.

Arnold, L.J., Bailey, R.M., Tucker, G.E., 2007. Statistical treatment of fluvial dose distributions from southern Colorado arroyo deposits. *Quaternary Geochronology* **2**, 162–167.

Bartyik, T., Magyar, G., Filyó, D., Tóth, O., Blanka-Végi, V., Kiss, T., Marković, S., et al., 2021. Spatial differences in the luminescence sensitivity of quartz extracted from Carpathian Basin fluvial sediments. *Quaternary Geochronology* **64**, 101166. https://doi.org/10.1016/j.quageo.2021.101166.

Bernat Rebollal, M., Pérez-González, A., 2008. Inland aeolian deposits of the Iberian Peninsula: Sand dunes and clay dunes of the Duero Basin and the Manchega Plain. Palaeoclimatic considerations. *Geomorphology* **102**, 207–220.

Bertran, P., Sitzia, L., Banks, W.E., Bateman, M.D., Demars, P.Y., Hernandez, M., Lenoir, M., Mercier, N., Prodeo, F., 2013. The Landes de Gascogne (southwest France): periglacial desert and cultural frontier during the Palaeolithic. *Journal of Archaeological Science* **40**, 2274–2285.

Borsy, Z., 1991. Blown sand territories in Hungary. *Zeitschrift für Geomorphologie Supplementary Issues* **90**, 1–14.

Borsy, Z., 1990. Evolution of the alluvial fans of the Alföld. In: Rachocki, A.H., Church, M. (Eds.), *Alluvial Fans. A Field Approach*. Wiley, Chichester. pp. 229–245.

Bøtter-Jensen, L., Thomsen, K.J., Jain, M., 2010. Review of optically stimulated luminescence (OSL) instrumental developments for retrospective dosimetry. *Radiation Measurements* **45**, 253–257.

Brennan, B.J., 2003. Beta doses to spherical grains. *Radiation Measurements* **37**, 299–303.

Bukurov, B., 1954. Geomorfološke prilike Banatskog Podunavlja [The geomorphological circumstances of the Banat Danube Basin]. *Journal of the Geographical Institute "Jovan Cvijić" SASA* **8**, 55–87. [in Serbian]

Bukurov, B., 1982. Sintetička razmatranja geomorfoloških problema na teritoriji Vojvodine [Synthetic approach of geomorphological issues in Vojvodina]. *Vojvođanska Akademija Nauka i Umetnosti* **5**, 1–97. [in Serbian]

Bulur, E., 1996. An alternative technique for optically stimulated luminescence (OSL) experiment. *Radiation Measurements* **26**, 701–709.

Buró, B., Sipos, Gy., Lóki, J., Andrási, B., Félegyházi, E., Négyesi, G., 2016. Assessing Late Pleistocene and Holocene phases of aeolian activity on the Nyírség alluvial fan, Hungary. *Quaternary International* **425**, 183–195.

Cholnoky, J., 1902. A futóhomok mozgásának törvényei. *Földtani Közlöny* **32**, 6–38. [in Hungarian]

Cholnoky, J., 1910. Az Alföld felszine. *Földrajzi Közlemények* **38**, 413–437. [in Hungarian]

Cholnoky, J., 1940. A futóhomok elterjedése. *Földtani Közlöny* **70**, 258–294. [in Hungarian]

Collins, W.D., Bitz, C.M., Blackmon, M.L., Bonan, G.B., Bretherton, C.S., Carton, J.A., Chang P., et al., 2006. The Community Climate System Model Version 3 (CCSM3), *Journal of Climate* **19**, 2122–2143.

Dietze, M., Kreutzer, S., Burow, C., Fuchs, M.C., Fischer, M., Schmidt, C., 2016, The abanico plot: visualising chronometric data with individual standard errors. *Quaternary Geochronology* **31**, 12–18.

Duller, G.A.T., 2003. Distinguishing quartz and feldspar in single grain luminescence measurements. *Radiation Measurements* **37**, 161–165.

Fábián, S.Á., Kovács, J., Varga, G., Sipos, G., Horváth, Z., Thamó-Bozsó, E., Tóth, G., 2014. Relict permafrost features in the Pannonian Basin, Hungary. *Boreas* **43**, 722–732.

Feurdean, A., Klotz, S., Brewer, S., Mosbrugger, V., Tămaş, T., Wohlfarth, B., 2008. Lateglacial climate development in NW Romania—comparative results from three quantitative pollen-based methods. *Palaeogeography Palaeoclimatology Palaeoecology* **265**, 121–133.

Feurdean, A., Perşoiu, A., Tanţău, I., Stevens, T., Magyari, E.K., Onac, B.P., Marković, S., et al., 2014. Climate variability and associated vegetation response throughout Central and Eastern Europe (CEE) between 60 and 8 ka. *Quaternary Science Reviews* **106**, 206–224.

Fordham, D.A., Saltré, F., Haythorne, S., Wigley, T.M.L., Otto-Bliesner, B.L., Chan, K.C., Brook, B.W., 2017. PaleoView: a tool for generating continuous climate projections spanning the last 21,000 years at regional and global scales. *Ecography* **40**, 1348–1358.

Gábris, Gy., 2003. A földtörténet utolsó 30 ezer évének szakaszai és a futóhomok mozgásának főbb periódusai Magyarországon (The periods of the history of the Earth for the last 30 thousand years and the most

important periods of movement of aeolian sand). *Földrajzi Közlemények* **127**, 1–13. [in Hungarian with English abstract]

Galbraith, R.F., Roberts, R.G., Laslett, G.M., Yoshida, H., Olley, J.M., 1999. Optical dating of single grains of quartz from Jinmium rock shelter, northern Australia: Part I, experimental design and statistical models. *Archaeometry* **41**, 339–364.

Gavrilov, M.B., Marković, S.B., Schaetzl, R.J., Tošić, I., Zeeden, C., Obreht, I., Sipos, Gy., et al., 2018. Prevailing surface winds in Northern Serbia in the recent and past time periods; modern- and past dust deposition. *Aeolian Research* **31**, 117–129.

Györgyövics, K., Kiss, T., 2016. Landscape metrics applied in geomorphology: hierarchy and morphometric classes of sand dunes in Inner Somogy, Hungary. *Hungarian Geographical Bulletin* **65**, 271–282.

Hesse, P.P., 2016. How do longitudinal dunes respond to climate forcing? Insights from 25 years of luminescence dating of the Australian desert dunefields. *Quaternary International* **410**, 11–29.

Hilgers, A., 2007. *The chronology of Late Glacial and Holocene dune development in the northern Central European lowland reconstructed by optically stimulated luminescence (OSL) dating*. PhD dissertation, Universität zu Köln, Germany.

Hrnjak, I., Lukić, T., Gavrilov, M.B., Marković, S.B., Unkašević, M., Tosić, I., 2014. Aridity in Vojvodina, Serbia. *Theoretical and Applied Climatology* **115**, 323–332.

Hugenholtz, C.H., Bender, D., Wolfe, S., 2010. Declining sand dune activity in the southern Canadian prairies: historical context, controls and ecosystem implications. *Aeolian Research* **2**, 71–82.

Jain, M., Murray, A.S., Bøtter-Jensen, L., 2003. Characterisation of blue-light stimulated luminescence components in different quartz samples: implications for dose measurement. *Radiation Measurements* **37**, 441–449.

Kalińska-Nartiša, E., Thiel, C., Nartišs, M., Buylaert, J.P., Murray, A.S., 2016. The north-eastern aeolian 'European Sand Belt' as potential record of environmental changes: A case study from Eastern Latvia and Southern Estonia. *Aeolian Research* **22**, 59–72.

Kasse, C.K., 2002. Sandy aeolian deposits and environments and their relation to climate during the Last Glacial Maximum and Lateglacial in northwest and central Europe. *Progress in Physical Geography: Earth and Environment* **26**, 507–532.

Kiss, T., Sipos, Gy., Kovács, F., 2009. Human impact on fixed sand dunes revealed by morphometric analysis. *Earth Surface Processes and Landforms* **34**, 700–711.

Kiss, T., Györgyövics, K., Sipos, Gy., 2012a. Homokformák morfológiai tulajdonságainak és korának vizsgálata Belső-Somogy területén (Morphometry and age of sand dunes in Inner Somogy, Hungary). *Földrajzi Közlemények* **136**, 361–375. [in Hungarian with English abstract]

Kiss, T., Sipos, Gy., Mauz, B., Mezősi, G., 2012b. Holocene aeolian sand mobilization, vegetation history and human impact on the stabilized sand dune area of the southern Nyírség, Hungary. *Quaternary Research* **78**, 492–501.

Kreutzer, S., Schmidt, C., Fuchs, M.C., Dietze, M., Fischer, M., Fuchs, M., 2012. Introducing an R package for luminescence dating analysis. *Ancient TL* **30**, 1–8.

Li, Y., Zhang, W., Aydin, A., Deng, X., 2018. Formation of calcareous nodules in loess—paleosol sequences: Reviews of existing models with a proposed new "per evapotranspiration model." *Journal of Asian Earth Sciences* **154**, 8–16.

Liritzis, I., Stamoulis, K., Papachristodoulou, C., Ioannides, K., 2013. A re-evaluation of radiation dose-rate conversion factors. *Mediterranean Archaeology and Archaeometry* **13**, 1–15.

Lóki, J., 1981. Belső-Somogy futóhomok területeinek kialakulása és formái (The development and forms of the blown sand areas of Belső-Somogy). *Acta Geographica ac Geologica et Meteorologica Debrecina* **18–19**, 81–111. [in Hungarian]

Ludwig, P., Gavrilov, M.B., Radaković, M.G., Marković, S.B., 2021. Malaco temperature reconstructions and numerical simulation of environmental conditions in the southeastern Carpathian Basin during the Last Glacial Maximum. *Journal of Quaternary Science*. https://doi.org/10.1002/jqs.3318.

Magyari, E.K., Pál, I., Vincze, I., Veres, D., Jakab, G., Braun, M., Szalai, Z., Szabó, Z., Korponai, J., 2019. Warm Younger Dryas summers and early late glacial spread of temperate deciduous trees in the Pannonian Basin during the last glacial termination (20–9 kyr cal BP). *Quaternary Science Reviews* **225**, 105980. https://doi.org/10.1016/j.quascirev.2019.105980.

Marković-Marjanović, J., 1950. Prethodno saopštenje o Deliblatsoj peščari (Preliminary results concerning the Deliblatska Peščara). *Zbornik radova Geološkog instituta SAN* **1**, 75–90. [in Serbian]

Mátyus, L., 1870. *Österreichische Monatsschrift für Forstwesen* **19–20**, p. 45. [in German]

Mauri, A., Davis, B.A.S., Collins, P.M., Kaplan, J.O., 2015. The climate of Europe during the Holocene: a gridded pollen-based reconstruction and its multi-proxy evaluation. *Quaternary Science Reviews* **112**, 109–127.

Mauz, B., Bode, T., Mainz, E., Blanchard, H., Hilger, W., Dikau, R., Zöller, L., 2002. The luminescence dating laboratory at the University of Bonn: Equipment and procedures. *Ancient TL* **20**, 53–61.

Menković, L., 2013. Eolian relief of southeast Banatian. *Bulletin of Serbian Geographical Society* **93**, 1–12.

Mezősi, G., 2017. *The Physical Geography of Hungary*. Springer International Publishing, Cham.

Moska, P., Sokołowski, R.J., Jary, Z., Zieliński, P., Raczyk, J., Szymak, A., Krawczyk, M., et al., 2021. Stratigraphy of the Late Glacial and Holocene aeolian series in different sedimentary zones related to the Last Glacial maximum in Poland. *Quaternary International*. https://doi.org/10.1016/j.quaint.2021.04.004.

Muhs, D.R., Holliday, V.T., 1995. Evidence of active dune sand on the Great Plains in the 19th century from accounts of early explorers. *Quaternary Research* **43**, 198–208.

Murray, A.S., Wintle, A.G., 2003. The single aliquot regenerative dose protocol: potential for improvements in reliability. *Radiation Measurements* **37**, 377–381.

Novothny, Á., Frechen, M., Horváth, E., 2010. Luminescence dating of periods of sand movement from the Gödöllő Hills, Hungary. *Geomorphology* **122**, 254–263.

Nyári, D., Kiss, T., Sipos, Gy, 2007. Investigation of Holocene blown-sand movement based on archaeological findings and OSL dating, Danube-Tisza Interfluve, Hungary. *Journal of Maps* **3**, 46–57.

Perşoiu, A., Onac, B.P., Wynn, J.G., Blaauw, M., Ionita, M., Hansson, M., 2017. Holocene winter climate variability in Central and Eastern Europe. *Scientific Reports* **7**, 1196.

Prescott, J.R., Hutton, J.T., 1994. Cosmic ray contributions to dose rates for luminescence and ESR dating: large depths and long-term time variations. *Radiation Measurements* **23**, 497–500.

Rasmussen, S.O., Bigler, M., Blockley, S.P., Blunier, T., Buchhardt, S.L., Clausen, H.B., Cvijanovic, I., et al., 2014. A stratigraphic framework for abrupt climatic changes during the Last Glacial period based on three synchronized Greenland ice-core records: refining and extending the INTIMATE event stratigraphy. *Quaternary Science Reviews* **106**, 14–28.

Roth, J. 1916. Die Aufforstungen der Ungarischen Flugsandgebiete. *Forftwiffenfchaftliches Centralblatt* **38**, 464–487.

Shakun, J.D., Carlson, A.E., 2010. A global perspective on Last Glacial Maximum to Holocene climate change. *Quaternary Science Reviews* **29**, 1801–1816.

Singarayer, J.S., Bailey, R.M., 2003. Further investigations of the quartz optically stimulated luminescence components using linear modulation. *Radiation Measurements* **37**, 451–458.

Sipos, G., Marković, S., Tóth, O., Gavrilov, M., Balla, A., Kiss, T., Urdea, P., Mészáros, M., 2016. *Assessing the morphological characteristics and formation time of the Deliblato Sands, Serbia*. Geophysical Research Abstracts 18, EGU General Assembly 2016, 17–22 April, Vienna.

Sümegi, P., Molnár, M., Jakab, G., Persaits, G., Majkut, P., Páll, D.G., Gulyás, S., Jull, A.T., Törőcsik, T., 2011. Radiocarbon-dated paleoenvironmental changes on a lake and peat sediment sequence from the central Great Hungarian Plain (central Europe) during the last 25,000 years. *Radiocarbon* **53**, 85–97.

Sümegi, P., Magyari, E., Daniel, P., Molnár, M., Törőcsik, T., 2013. Responses of terrestrial ecosystems to Dansgaard–Oeshger cycles and Heinrich-events: a 28,000-year record of environmental changes from SE Hungary. *Quaternary International* **293**, 34–50.

Telfer, M.W., Hesse, P.P., 2013. Palaeoenvironmental reconstructions from linear dunefields: recent progress, current challenges and future directions. *Quaternary Science Reviews* **78**, 1–21.

Tolksdorf, J.F., Kaiser, K., 2012. Holocene aeolian dynamics in the European sand-belt as indicated by geochronological data. *Boreas* **41**, 408–421.

Tóth, M., Magyari, E.K., Brooks, S.J., Braun, M., Buczkó, K., Bálint, M., Heiri, O., 2012. A chironomid-based reconstruction of late glacial summer temperatures in the southern Carpathians (Romania). *Quaternary Research* **77**, 122–131.

Tóth, O., Sipos, Gy., Kiss, T., Bartyik, T., 2017. Variation of OSL residual doses in terms of coarse and fine grain modern sediments along the Hungarian section of the Danube. *Geochronometria* **44**, 319–330.

Ujházy, K., Gábris, Gy., Frechen, M., 2003. Ages of periods of sand movement in Hungary determined through luminescence measurements. *Quaternary International* **111**, 91–100.

Unkašević, M., Tošić, I., Obradović, M., 2007. Spectral analysis of the "Koshava" wind. *Theoretical and Applied Climatology* **89**, 239–244.

Vandenberghe, D.A.G., Derese, C., Kasse, C., Van den Haute P., 2013. Late Weichselian (fluvio-)aeolian sediments and Holocene drift-sands of the classic type locality in Twente (E Netherlands): a high-resolution dating study using optically stimulated luminescence. *Quaternary Science Reviews* **68**, 96–113.

Wintle, A.G., and Murray, A.S., 2006. A review of quartz optically stimulated luminescence characteristics and their relevance in single-aliquot regeneration dating protocols. *Radiation Measurements* **41**, 369–391.

Zeremski, M., 1972. Južnobanatska lesna zaravan-prilog regionalnoj geomorfologiji iz aspekta egzo i endodinamičkih procesa. The Southern Banat plateau (toward a regional geomorphology of Vojvidina—exo- and endodynamic processes). *Zbornik za Prirodne Nauke* **43**, 5–80. [in Serbian]